

INTTRAVEL: A REAL-WORLD DATASET AND GENERATIVE FRAMEWORK FOR INTEGRATED MULTI-TASK TRAVEL RECOMMENDATION

Huimin Yan*, Longfei Xu*, Junjie Sun, Zheng Liu,

Wei Luo, Kaikui Liu, Xiangxiang Chu

AMAP, Alibaba Group

ABSTRACT

Next Point of Interest (POI) recommendation is essential for modern mobility and location-based services. To provide a smooth user experience, models must understand several components of a journey holistically: “when to depart”, “how to travel”, “where to go”, and “what needs arise via the route”. However, current research is limited by fragmented datasets that focus merely on next POI recommendation (“where to go”), neglecting the departure time, travel mode, and situational requirements along the journey. Furthermore, the limited scale of these datasets impedes accurate evaluation of performance. To bridge this gap, we introduce **IntTravel**, the first large-scale public dataset for integrated travel recommendation, including **4.1 billion interactions from 163 million users with 7.3 million POIs**. Built upon this dataset, we introduce an end-to-end, **decoder-only generative framework for multi-task recommendation**. It incorporates information preservation, selection, and factorization to balance task collaboration with specialized differentiation, yielding substantial performance gains. The framework’s generalizability is highlighted by its state-of-the-art performance across both IntTravel dataset and an additional non-travel benchmark. IntTravel has been successfully deployed on Amap serving hundreds of millions of users, leading to a 1.09% increase in CTR. IntTravel is available at <https://github.com/AMAP-ML/IntTravel>.

1 INTRODUCTION

Next POI (Point of Interest) prediction is crucial for location-based service platforms. Accurate prediction of the next POI allows for the provision of excellent service to billions of users. Except for next POI prediction, a truly seamless service requires modeling of a user’s intents across multiple dimensions: when to depart, where to go, how to travel, and what needs arise via the route.

However, we find that existing datasets (Cho et al., 2011; Cheng et al., 2011; Yang et al., 2014; 2016; Monti et al., 2018; Yang et al., 2019) in the field of travel-related recommendation face two significant limitations (see Table 1 for dataset comparison). **Most datasets are generated and processed for next POI recommendation**, while ignoring the relationships between destination, departure time, travel mode, and on-the-way intentions of users. Furthermore, **the insufficient scale of these datasets hinders accurate evaluations of generative models**, potentially leading to incorrect findings. To bridge these gaps, we introduce **IntTravel**, a comprehensive dataset for multi-task travel recommendation. It is built on large-scale dataset collected from a leading provider of digital map, navigation and real-time traffic information in China. IntTravel covers four core tasks to capture the entire journey of a user:

- **When (departure time)**: Predicting the time a user intends to start a journey.
- **Where (destination)**: Recommending the POI the user aims to reach in his/her next journey.

*Equal contribution.

[†]Corresponding author.

Table 1: Comparison of different datasets.

Datasets	# Users	# Interactions	Data			
			POI check-in	Time feature	Travel mode	Waypoints
Cheng et al. (2011)	224,804	22,388,315	✓	✓	✗	✗
Cho et al. (2011)	196,591	6,442,890	✓	✓	✗	✗
Yang et al. (2014)	2,763	801,131	✓	✓	✗	✗
Yang et al. (2016)	266,909	33,278,683	✓	✓	✗	✗
Monti et al. (2018)	424,730	12,473,360	✓	✓	✗	✗
Yang et al. (2019)	114,324	22,809,624	✓	✓	✗	✗
IntTravel (ours)	163 M	4.1 B	✓	✓	✓	✓

- **How (travel mode):** Determining the preferred mode, such as driving, walking, or public transit.
- **Via (on-the-way intention):** Predicting the on-the-way POI a user is likely to visit while traveling toward a confirmed destination.

Recently, models for next POI prediction have transitioned from traditional deep learning architectures to generative paradigms (Li et al., 2024; Wang et al., 2024; 2025a; Wei et al., 2025). Generative models (Rajput et al., 2023b; Zhai et al., 2024b; Yan et al., 2025; Deng et al., 2025b) replace the traditional multi-stage recommendation pipeline of recall, pre-ranking, ranking and re-ranking. They also eliminate the need for complex feature engineering by automatically learning from raw data. Decoder-only generative models achieve comparable or even better performance than traditional deep learning based models.

Nevertheless, traditional multi-task frameworks are incompatible with generative architectures. This is mainly because **sequence representation has evolved from an important feature into the primary driver for next-token generation**. Traditional methods process tasks after combining information, which means they fail to maintain task-specific independence within the Transformer’s encoding layers. To tackle this issue, we introduce **IntTravel**, the first multi-task generative framework for end-to-end travel recommendation. The architecture is built upon three primary components: (1) **Multi-task Information Preservation**: This module enriches hyper-connections with task-specific properties, thereby streamlining the delivery of information across the architecture and ensuring its integrity. (2) **Multi-task Information Selection**: This module employs selective gating across hidden layers to retrieve multi-scale, task-specific information tailored to different encoding levels. (3) **Multi-task Information Factorization**: This module combines the outputs of the preservation and filtering stages. It uses shared and separate parameters among experts to balance common knowledge with specific task needs.

Comprehensive offline experiments demonstrate that IntTravel consistently outperforms all existing deep learning based multi-task baselines on the IntTravel dataset. For versatility evaluation, we further conducted experiments on an additional non-travel benchmark, where IntTravel also achieved state-of-the-art results. The framework has been fully deployed within Amap, powering services such as personalized POI recommendations and travel mode suggestions. We provide this dataset and framework to drive the development of generative foundation models for multi-task recommendation.

In summary, we summarize our contributions as follows:

- **Real-world industrial dataset:** We introduce IntTravel, a large-scale, real-world dataset that integrates four key travel tasks (When, How, Where, and Via).
- **Generative multi-task framework:** We design IntTravel, a multi-task decoder-only framework that integrating four travel tasks as a joint sequence generation problem, enabling end-to-end optimization.
- **Offline demonstrations and online deployment:** We validated IntTravel using both public and industrial datasets. IntTravel has been successfully deployed online.

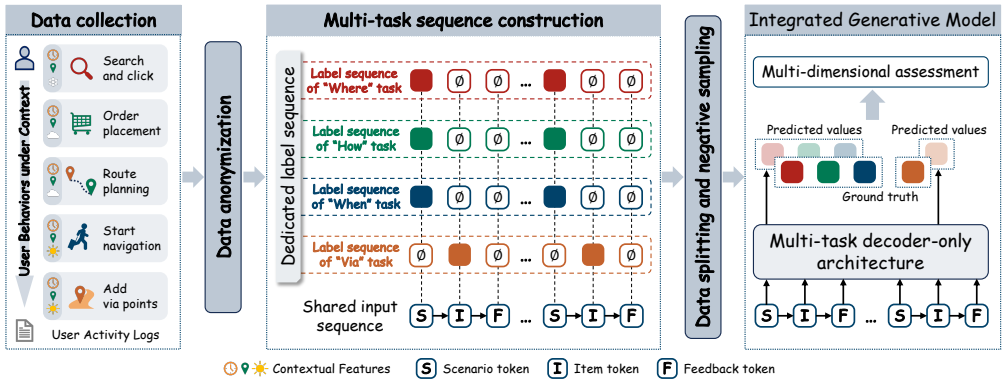


Figure 1: The end-to-end pipeline of IntTravel. The workflow processes raw, contextual user logs by tokenizing them into a unified, multi-task sequence format, which includes a shared input sequence and dedicated label sequences for four distinct travel tasks. This structured data is then fed into a decoder-only generative model that jointly predicts all task outcomes, with performance evaluated via a comprehensive multi-dimensional assessment.

2 RELATED WORKS

2.1 TRAVEL DATASETS

Travel planning is a complex real world challenge that involves several key subtasks: POI discovery, transportation and route optimization, and the creation of travel plans for both short-term and long-distance travel. To tackle these challenges, increasing research utilizes AI agents to manage constraints, decompose objectives, and optimize plans through iterative refinement and tool integration. In response, datasets and benchmarks (Xie et al., 2024; Wang et al., 2025b; Hao et al., 2025) have been developed to evaluate agent performance. However, in many real-world travel application scenarios, there is a pressing need to accurately predict a user’s next journey across four fundamental dimensions: departure timing (when), transportation mode (how), destination (where), and situational needs (via). In this context, existing datasets (Yang et al., 2014; Cho et al., 2011; Cheng et al., 2011) focus exclusively on Next-POI recommendation (where to go), neglecting the temporal, modal, and situational requirements of a journey. Given the current paradigm shift toward generative recommendation, the limited scale of these datasets results in inadequate evaluation of generative models.

2.2 MULTI-TASK LEARNING

Multi-task learning (MTL) models have evolved significantly, moving from simple shared structures to more adaptive architectures. Early models, such as the classic Shared-Bottom (Caruana, 1997), used a hard parameter sharing approach with common bottom layers. However, this often led to negative transfer when tasks were not closely related. To address this, soft parameter sharing models emerged. MMoE (Ma et al., 2018) introduced task-specific gates to flexibly combine shared experts. PLE (Tang et al., 2020) further improved this by explicitly separating shared and task-specific experts, effectively mitigating the “seesaw phenomenon.” As systems grew to serve multiple scenarios, the focus expanded. Models like STAR (Sheng et al., 2021), M2M (Zhang et al., 2022), and HiNet (Zhou et al., 2023) developed specialized architectures to explicitly manage inter-scenario relationships. More recently, the granularity of sharing has advanced to the embedding level. STEM-Net (Su et al., 2024) pioneers learning both shared and task-specific embeddings to capture diverse user preferences.

2.3 GENERATIVE RECOMMENDATION

Generative Recommendation (GR) transforms traditional retrieval into sequence generation (Geng et al., 2022; Zheng et al., 2024; Liu et al., 2025; Xu et al., 2025). In contrast to traditional deep-learning-based models, generative recommenders possess the potential to alleviate cascaded error

propagation and facilitate optimization across broader user behavioral contexts. TIGER (Rajput et al., 2023a) first predicted hierarchical SIDs via a sequence-to-sequence model, while HSTU (Zhai et al., 2024a) unified retrieval and ranking by interleaving item and action tokens. IntSR (Yan et al., 2025) further integrated search and recommendation through a query-driven block that isolates query placeholders from user history. OneRec (Deng et al., 2025a) replaced multi-stage pipelines with an end-to-end generative architecture. However, research addressing multi-task learning within the generative paradigm remains scant.

3 PRELIMINARY

Let \mathcal{U} be the set of users and \mathcal{I} be the set of POIs. \mathcal{A} is the set of all user interactions. For each user $u \in \mathcal{U}$, their historical travel behavior is represented as a chronological sequence of interactions $\mathcal{A}_u = (i_1, i_2, \dots, i_N)$, where each interaction contains contextual information such as the visited POI, the chosen travel mode, and timestamp. N is length of this sequence.

Let \mathcal{K} be the set of all tasks. Our goal is to build a multi-task generative model that, given a user’s historical interaction sequence, simultaneously predicts the recommendation result for each task $k \in \mathcal{K}$ for his/her next journey. All tasks share the same input sequence \mathcal{A}_u . The training objective is to find the optimal set of model parameters, Θ , that maximizes the log-likelihood of observing the ground-truth labels for all tasks across the entire training dataset \mathcal{D} . This can be formally expressed as:

$$\hat{\Theta} = \arg \max_{\Theta} \sum_{(\mathcal{A}, \mathbf{y}) \in \mathcal{D}} \log P([y_k | k \in \mathcal{K}] | \mathcal{A}; \Theta), \quad (1)$$

where y_k represents the ground-truth label of task k .

4 INTTRAVEL: DATASET

IntTravel is a comprehensive real-world dataset for multi-task travel recommendation, including 163 million users, 7.3 million POIs, and 4.1 billion of user actions. Figure 1 presents the pipeline of IntTravel to convert raw data of diverse user behaviors into structured input sequence of recommendation models.

4.1 DATA COLLECTION

All data are collected from a leading provider of digital map, navigation and real-time traffic information in China. Data collection is strictly confined to in-app logs and explicitly excludes all personally identifiable information. These operational logs, spanning a 90-day period across several major cities in China, record the following types of user behaviors: (1) Search and click actions of POIs within the application. (2) Ordering actions for a specific POI (e.g., purchasing a service or a dining coupon). (3) Route planning, including the selected mode of travel. (4) Navigation initiation, including the selected mode of travel. (5) Search and addition of via POIs along the route. Data examples and statistics can be found in Appendix A.

4.2 USER PROFILE ANONYMIZATION

To preserve privacy, we release only the processed IDs or transcoded information and do not include any raw data. For user profile data, original user IDs were replaced with randomly generated IDs. The original names of the six profile features in the released dataset are now represented by generic labels, such as “profile feature 1” and “profile feature 2”. Additionally, the values for each feature were mapped to discrete, consecutive integer IDs. This mapping makes it impossible for data users to infer the real-world meaning of any ID. The raw latitude and longitude data have been transformed. While the resulting coordinates preserve the original relative positioning, the distance may be inaccurate. This prevents identifying the users’ actual physical locations. The dataset also contains geographical block IDs mapped from the raw coordinates.

4.3 MULTI-TASK SEQUENCE CONSTRUCTION

The construction of input sequence adopts a structure similar to that of IntSR (Yan et al., 2025). Since our focus is on the recommendation retrieval problem, we omit the Q (query) tokens. Specifically, the input sequence comprises three types of tokens:

- **S (Scenario tokens):** These tokens encode the spatiotemporal context of user activities, allowing the model to learn context-aware user preferences.
- **I (Item tokens).** These tokens form the chronological backbone of a user’s interaction history. Each token corresponds to a POI the user has interacted with.
- **F (Feedback tokens).** Paired with each item token, these tokens explicitly signal the user’s interaction type, such as a “click” or an “order”. These tokens provide crucial information about the intensity and type of user engagement, enriching the model’s understanding of user intent.

Multiple tasks share the same input sequence, while each task is supervised by a dedicated label sequence. To prevent data leakage in our chronologically ordered input, we strategically attach labels to specific token types based on the predictive goal of each task.

For the “When,” “How,” and “Where” tasks, labels are attached to the S tokens. This forces the model to make predictions using only the current context and past interactions. For the “Via” task, which focuses on predicting on-the-way intent, its labels are anchored to the I tokens, conditioning the prediction on a known destination. For any given task, tokens not relevant for its supervision are assigned a null label. This label attachment strategy is illustrated in the middle of Figure 1. It works in conjunction with our decoder-only architecture and its inherent causal masking mechanism to strictly prevent information leakage.

4.4 DATASET SPLITTING

For the full IntTravel dataset, we adopted a temporal splitting strategy. For each user, all interactions, excluding the last two, were used to form the training set. The penultimate interaction was designated as the validation set, and the final served as the test set. However, due to the large size of the dataset, we constructed the validation and test sets by randomly sampling 5% from the whole dataset, which amounts to approximately 815,000 interactions.

4.5 NEGATIVE SAMPLING

Regarding the construction of negative samples, no sampling was required for the “when” and “how” tasks, as their candidate sets are small. For the “where” and “via” tasks, which involve a vast number of POIs, we employed a hybrid negative sampling strategy. This strategy combines uniform random sampling with location-based hard negative sampling. Specifically, for each action, we constructed the negative set by:

- Randomly sampling 14 POIs from the entire POI corpus (excluding the ground truth).
- Distance-based negative sampling is not applicable because the original latitude and longitude coordinates have been processed. Therefore, hard negative samples are obtained by sampling 50 POIs from the same geographic ID (also excluding the ground truth). If fewer than 50 such POIs were available, all of them were included.

5 INTTRAVEL: MULTI-TASK GENERATIVE FRAMEWORK

IntTravel proposes a bottom-up multi-task method to handle multiple tasks within a single generative model, as presented in Figure 2. The approach comprises three modules:

- **Task-Guided Information Persistence (TIP)** ensures maximum propagation of task-relevant information in the decoder while keeping the computational complexity at $\mathcal{O}(N^2C)$.

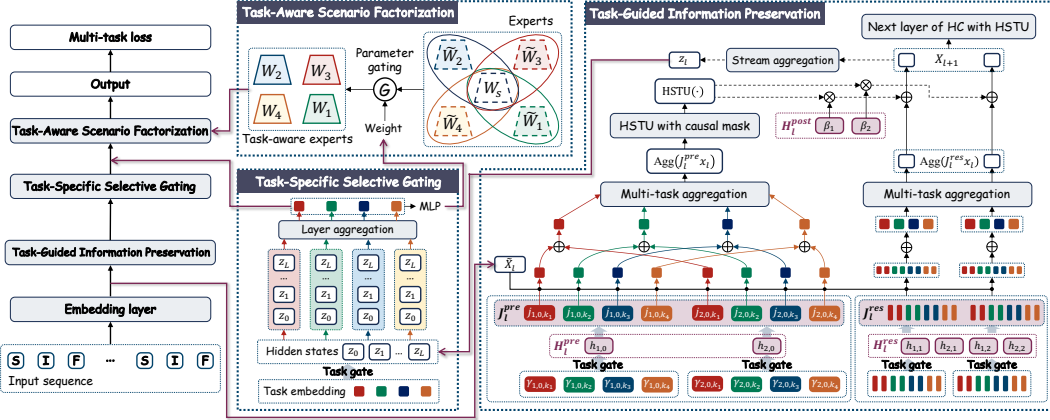


Figure 2: Multi-task framework of IntTravel. IntTravel stacks three core modules to handle multiple tasks. Task-Guided Information Preservation (TIP) ensures task-relevant information is retained. Task-Specific Selective Gating (TSG) filters useful information for each task. Task-Aware Scenario Factorization (TSF) generates task-aware parameters for the output.

- **Task-Specific Selective Gating (TSG)** enables each task to filter useful information from the decoder’s output.
- **Task-Aware Scenario Factorization (TSF)** empowers each task to factorize its output based on specific scenarios.

5.1 TASK-GUIDED INFORMATION PERSISTENCE (TIP)

5.1.1 HSTU

Hierarchical Sequential Transduction Unit (HSTU) (Zhai et al., 2024a) is a decoder-only architecture widely used in generative recommendation (Yan et al., 2025; Han et al., 2025). It stacks multiple uniform layers with residual connections. Each layer of HSTU is formulated in Eqs. (2)-(3), where $x_l, x_{l+1} \in \mathbb{R}^C$ denote the input and output of the l_{th} layer. U_l, V_l, Q_l , and K_l are gating weights, values, queries, and keys, respectively. Positional and temporal relative bias, rab^p and rab^t , are introduced to refine the similarity scores. f_1 and f_2 are linear layers. Causal mask is applied in HSTU to prevent information leakage.

$$U_l, V_l, Q_l, K_l = \text{Split}(\text{SiLU}(f_1(x_l))), \quad (2)$$

$$x_{l+1} = f_2 \left(\text{Norm} \left(Q_l^\top K_l + \text{rab}^p + \text{rab}^t \right) V_l \right) \odot U_l. \quad (3)$$

5.1.2 TIP

TIP module is the multi-task version of Hyper Connection (HC) embedded with HSTU as decoder, enabling both the advantages of residual connection expansion and the maximal preservation of task-aware information. HC has been validated effective by expands the width of residual stream without introducing much computation overhead (Zhu et al.). The mechanism of HC can be defined as Eq. (4).

$$X_{l+1} = H_l^{\text{res}} X_l + (H_l^{\text{post}})^\top F(H_l^{\text{pre}} X_l, W_l). \quad (4)$$

X_l and X_{l+1} denote the input and output of the l_{th} layer with hyper connection. With expansion rate denoted by n , $X_l, X_{l+1} \in \mathbb{R}^{n \times C}$, where C is feature dimension. The initial hyper connection input is formed by replicating the network input for n times, i.e., $X_0 = [x_0 \ x_0 \dots \ x_0]^\top \in \mathbb{R}^{n \times C}$. $H_l^{\text{pre}} \in \mathbb{R}^{1 \times n}$ aggregates features from n streams, X_l , into one combined stream; $H_l^{\text{post}} \in \mathbb{R}^{1 \times n}$ expands the output back to n streams. $H_l^{\text{res}} \in \mathbb{R}^{n \times n}$ serves as the mixing parameters of residual streams. F represents any network layer, such as attention mechanisms or feed forward networks.

HC is static when H_l^{pre} , H_l^{post} , and H_l^{res} are initialized as learnable parameters, i.e., $b_l^{\text{pre}}, b_l^{\text{post}} \in \mathbb{R}^{1 \times n}$, $b_l^{\text{res}} \in \mathbb{R}^{n \times n}$. In dynamic HC, H_l^{pre} , H_l^{post} , and H_l^{res} are calculated as the summation of dynamic part and static part, as shown in Eq. (5). The static part is same as that of static HC, while the dynamic part depends on the input X_l . With input \tilde{X}_l , the dynamic part is derived by linear projections with parameters defined as $\theta_l^{\text{pre}}, \theta_l^{\text{post}} \in \mathbb{R}^{1 \times C}$ and $\theta_l^{\text{res}} \in \mathbb{R}^{n \times C}$. $\alpha_l^{\text{pre}}, \alpha_l^{\text{post}}, \alpha_l^{\text{res}} \in \mathbb{R}$ are learnable gating values.

$$\begin{cases} \tilde{X}_l = \text{RMSNorm}(X_l) \\ H_l^{\text{pre}} = \alpha_l^{\text{pre}} \cdot \tanh(\theta_l^{\text{pre}} \tilde{X}_l^\top) + b_l^{\text{pre}} \\ H_l^{\text{post}} = \alpha_l^{\text{post}} \cdot \tanh(\theta_l^{\text{post}} \tilde{X}_l^\top) + b_l^{\text{post}} \\ H_l^{\text{res}} = \alpha_l^{\text{res}} \cdot \tanh(\theta_l^{\text{res}} \tilde{X}_l^\top) + b_l^{\text{res}} \end{cases} \quad (5)$$

The standard HC is not designed for multi-task problems, and thus, is not capable of handling multiple tasks. We extend the standard hyper-connection to a multi-task version by incorporating a task-gating mechanism. As formulated in Eq. (6), the task-specific parameters, $J_{l,k}^{\text{pre}}$ and $J_{l,k}^{\text{res}}$, are generated for each task k . This is achieved by performing an element-wise product between the primary, task-agnostic parameters (H_l^{pre} and H_l^{res}) and a corresponding task-specific gate, $\gamma_{l,k}$. This gate acts as a dynamic filter, selectively scaling the shared primary parameters to create a customized set of parameters tailored to the specific needs of task k .

$$J_{l,k}^{\text{pre}} = H_l^{\text{pre}} \odot \gamma_{l,k}, J_{l,k}^{\text{res}} = H_l^{\text{res}} \odot \gamma_{l,k}. \quad (6)$$

Therefore, the multi-task version of HC with F instantiated as HSTU can be formulated as:

$$X_{l+1} = \text{Agg}(J_{l,k}^{\text{res}} X_l) + (H_l^{\text{post}})^\top \text{HSTU} \left(\text{Agg}(J_{l,k}^{\text{pre}} X_l), W_l \right), \quad (7)$$

where $\text{Agg}(\cdot)$ denotes an aggregation function to combine the information learned across all tasks. For example, a simple aggregation function could be to sum or average pooling over the task dimension k . In this way, the final results contain the collective information from all individual tasks.

5.2 TASK-SPECIFIC SELECTIVE GATING (TSG)

The purpose of TSG is to select task-specific information and to form the input of following scenario factorization network. The process involves three key steps. First, to create a unified representation for each decoder layer's output, the multi-stream output $x_l \in \mathbb{R}^{n \times C}$ from the preceding TIP layer is aggregated along stream dimension to obtain $z_l \in \mathbb{R}^C$, see Eq. (8).

$$z_l = \text{Agg}(X_l). \quad (8)$$

Second, to enable task-specific filtering, the module must determine the relevance of each layer's information for each task. To this end, a series of layer-specific gating scalars, $s_{l,k}$, are generated for each task k from its unique task embedding e_k via an MLP, as shown in Eq. (9). Each scalar $s_{l,k}$ learns to quantify the importance of layer l 's output for task k . With these importance scores, the module performs the selective gating. As formulated in Eq. (10), z_l is scaled by $s_{l,k}$ through an element-wise Hadamard product (\odot). This operation effectively filters the layer's information by amplifying features relevant to task k and suppressing irrelevant ones, resulting in a task-aware representation $z_{l,k}$.

$$s_{l,k} = \text{MLP}(e_k), \quad (9)$$

$$z_{l,k} = s_{l,k} \odot z_l. \quad (10)$$

Finally, to construct a single, comprehensive output for each task, the filtered, layer-specific representations $z_{l,k}$ are aggregated across all decoder layers l . This step combines the selected information from the entire decoder depth into the final task-specific output of the TSG module, z_k , as shown in Eq. (11). In our implementation, this aggregation is performed using average pooling.

$$z_k = \text{Agg}(z_{l,k}). \quad (11)$$

5.3 TASK-AWARE SCENARIO FACTORIZATION (TSF)

The Task-Aware Scenario Factorization (TSF) module is designed to handle different tasks and user preferences. This is achieved by dynamically creating customized MLP layers that adapt to each specific situation. Inspired by the concept of scenario-based parameter generation of DSFNet (Yu et al., 2025), we enhance this idea by introducing a clear distinction between shared and task-private experts for better multi-task learning. Specifically, we define two types of experts:

- A set of **shared experts**, \mathcal{E}^s , which contain general knowledge that is useful for all tasks.
- A set of **private experts**, \mathcal{E}_k^p , which hold specialized knowledge tailored to each individual task k .

To decide how much each expert should contribute for a given situation, we calculate a weight β_e for each expert e . For each task k , we construct a task-specific context representation R_k by concatenating the task embedding e_k with user profile features p (Eq. (12)). R_k is passed through an MLP with sigmoid function σ and multiplied by 2 to obtain β_e (Eq. (13)). This allows the weight to be greater than 1, enabling the model to amplify the influence of experts that are particularly important for the current context.

$$R_k = \text{concat}(e_k, p), \quad (12)$$

$$\beta_e = 2 * \sigma(\text{MLP}(R_k)). \quad (13)$$

These weights are then used to build the final parameters of task k , W_k and b_k . As shown in Eq. (14), the final parameters are a weighted sum of the base parameters (\tilde{W}_e and \tilde{b}_e) from a selected group of experts. For any given task k , we only sum over the shared experts (\mathcal{E}^s) and that specific task's own private experts (\mathcal{E}_k^p). This allows each task to effectively combine general, shared knowledge with its own unique, specialized knowledge. In this way, the TSF module constructs an MLP layer whose parameters are customized to both the specific task k and the current user profile p .

In parallel, we refine the task-specific input features z_k using a filtering mechanism. As shown in Eq. (15), a dynamic gate is generated from both z_k and the context representation R_k . This gate is then applied element-wise to z_k to produce the filtered features \tilde{z}_k . The final output for task k , \hat{y}_k , is obtained by applying this newly constructed MLP layer (with parameters W_k and b_k) to its corresponding input representation, \tilde{z}_k , as shown in Eq. (16).

$$W_k = \sum_{e \in \mathcal{E}^s \cup \mathcal{E}_k^p} \beta_e \tilde{W}_e, b_k = \sum_{e \in \mathcal{E}^s \cup \mathcal{E}_k^p} \beta_e \tilde{b}_e, \quad (14)$$

$$\tilde{z}_k = z_k \odot \sigma(\text{MLP}(\text{concat}(z_k, R_k))), \quad (15)$$

$$\hat{y}_k = W_k \tilde{z}_k + b_k. \quad (16)$$

5.4 LOSS FUNCTION

For each individual task, we compute its InfoNCE loss which maximizes the probability of the ground-truth item, i^+ , over the set of all candidates \mathcal{I}_k . The final multi-task loss L is then the sum of all individual task losses, as shown in Eq. (17).

$$L = \sum_{k \in \mathcal{K}} -\frac{1}{|\mathcal{A}|} \sum_{u \in \mathcal{U}} \sum_{a \in \mathcal{A}_u} \log \frac{\exp(\hat{y}_k^{i^+})}{\sum_{i \in \mathcal{I}_k} \exp(\hat{y}_k^i)}. \quad (17)$$

6 EXPERIMENTS

6.1 DATASETS, BASELINES, AND EVALUATION METRICS

Datasets. In addition to the IntTravel dataset proposed in this work, we selected a dataset from a non-travel domain, **Tenrec-QK-video**¹ (Yuan et al., 2022), to validate the effectiveness of our multi-task model. The statistical information for both datasets is summarized in Table 2. Tenrec

¹<https://tenrec0.github.io/>

Table 2: Statistics of the datasets.

Dataset	#Users	#Items	#Interactions			#Exposures
			Total	Mean	Median	
IntTravel	162,815,693	7,291,872	4,129,827,011	25	21	/
Tenrec-QK-video	5,022,750	3,753,436	154,448,378	31	21	493,458,970

is a public recommendation dataset, and QK-video is the sub-dataset for video recommendation. It includes four types of user behaviors: clicks, likes, shares, and follows, with an approximate ratio of **166:12:1.3:1**². In addition to these interactions, Tenrec-QK-video also contains a large volume of exposure records.

Baselines. We compare IntTravel to the following baselines: (1) **PLE** (Tang et al., 2020) separates shared and task-specific experts within a multi-level structure for progressive knowledge extraction. (2) **STAR** (Sheng et al., 2021) employs a star topology that combines a central shared network with multiple domain-specific networks. (3) **M2M** (Zhang et al., 2022) uses a meta-learning approach to generate network parameters from scenario knowledge, modeling cross-scenario correlations. (4) **APG** (Yan et al., 2022) dynamically generates customized parameters based on each individual data instance. (5) **MuSeNet** (Xu et al., 2023) learns implicit scenarios from data and applies a causal framework to mitigate scenario-induced bias. (6) **HiNet** (Zhou et al., 2023) uses a hierarchical structure that extracts scenario-level information before processing task-level features. (7) **STEM-Net** (Su et al., 2024) learns both shared and task-specific embeddings, using a special gate to isolate task-specific gradient updates. (8) **HoME** (Wang et al., 2025c) enhances mixture-of-experts stability through expert normalization, a hierarchical mask for task grouping, and specialized gating mechanisms.

Evaluation metrics. The four travel tasks are evaluated using metrics detailed in Appendix B, including positive indicators such as Accuracy (Acc) and Hit Rate (HR), and negative ones like Mean Absolute Error (MAE), Bad Case Rate (BCR), and Category Inconsistency Rate (CIR). We report top-1 and top-5 HR. For the CTR prediction problem on Tenrec-QK-video, AUC (Area Under Curve) is used as evaluation metrics.

6.2 IMPLEMENTATION DETAILS

For experiments on the IntTravel dataset, we set the embedding size to 96, the maximum sequence length to 120, and the batch size to 64. The model was trained using a learning rate of 1×10^{-3} . Unless otherwise specified (as in the scaling law experiments), the number of layers in TSP module was set to 3. All baseline models adopted these same hyperparameter settings. For TSF module, we set 2 shared experts and 1 private expert for each task. When implementing baseline models, we set the decoder to the original HSTU with the same number of layers. The TSG module was removed, and the TSF module was replaced by the respective baseline models, which served as the multi-task heads.

For the Tenrec-QK-video dataset, we frame the problem as a multi-task Click-Through Rate (CTR) prediction task. The objective is to predict whether a user will perform one of four actions on a given item: “click”, “like”, “share”, or “follow”. We construct sequences using up to 50 of a user’s positive interactions. Following the approach in Yuan et al. (2022), we sample negative feedback from the exposure data. The ratio of positive/negative samples is set to 1:1. For these negative samples, the labels of all four task are set to 0. Due to the inclusion of negative samples, the maximum sequence length for all experiments on this dataset is set to 200. Since Tenrec lacks contextual features (spatial or temporal), sequences are composed solely of Item (I) and Feedback (F) tokens, with all task labels attached to the Item tokens. The embedding size was set to 32, and the batch size to 64. We employed a 3-layer TSP module and a smaller learning rate of 1×10^{-5} . Similarly, we set 2 shared experts and 1 private experts for each task in TSF module. The implementation approach for baselines on this dataset is identical to that on the IntTravel dataset.

²The dataset contains 142,321,193 clicks, 10,141,195 likes, 1,128,312 shares, and 857,678 follows.

Table 3: Comparison with baseline models across all four travel tasks on IntTravel dataset. For metrics, \uparrow indicates higher is better, and \downarrow indicates lower is better. The best results are in boldface and the second best are underlined.

Model	“When” task		“How” task		“Where” task			“Via” task		
	Acc \uparrow	MAE \downarrow	Acc \uparrow	BCR \downarrow	HR@1 \uparrow	HR@5 \uparrow	CIR \downarrow	HR@1 \uparrow	HR@5 \uparrow	CIR \downarrow
PLE	0.8331	8.013	0.6746	<u>0.0725</u>	0.6412	0.8504	0.2787	0.6405	0.8497	0.2818
STAR	0.8333	8.000	0.6741	0.0734	<u>0.6493</u>	<u>0.8534</u>	<u>0.2725</u>	0.6520	0.8539	0.2737
M2M	0.8313	8.097	0.6552	0.0869	0.5611	0.8208	0.3266	0.5686	0.8255	0.3208
APG	0.8330	8.016	0.6697	0.0773	0.5922	0.8317	0.3017	0.5962	0.8354	0.3070
HiNet	0.8325	8.039	<u>0.6751</u>	0.0731	0.6144	0.8406	0.2956	0.6087	0.8379	0.3026
MuSeNet	0.8324	8.047	0.6572	0.0911	0.6296	0.8453	0.2684	<u>0.6564</u>	<u>0.8553</u>	<u>0.2708</u>
STEM-Net	0.8330	8.031	0.6723	0.0735	0.6278	0.8438	0.2800	0.6370	0.8487	0.2834
HoME	0.8328	8.025	0.6738	0.0730	0.6356	0.8483	0.2811	0.6365	0.8479	0.2839
IntTravel	0.8330	8.016	0.6756	0.0724	0.6582	0.8556	0.2560	0.6592	0.8561	0.2552

All models are trained using Adam optimizer (Adam et al., 2014) on 8 NVIDIA H20 GPUs with 96 GB memory.

6.3 OVERALL COMPARISONS

Performance on the IntTravel Dataset. As detailed in Table 3, our proposed IntTravel model demonstrates superior performance on its native travel-domain dataset. It consistently achieves state-of-the-art results, reaching the top or second-best position across the metrics for all four tasks. These results highlight the effectiveness of our architecture in capturing the relationships among travel-related predictions. Components like TIP and TSF allow the model to maintain crucial context and generate customized parameters for each specific travel scenario.

Generalization to a Non-Travel Domain. The results on Tenrec-QK-video are presented in Table 4. IntTravel outperforms all baseline models, including strong competitors like HoME and STEM-Net, across all four prediction tasks (click, like, share, and follow). It proves the robustness and generalizability of IntTravel architectural. The model’s ability to dynamically generate task-specific parameters (via TSF) and selectively filter information (via TSG) constitutes a effective mechanism that adapts well to diverse multi-task environments.

6.4 ABLATION STUDIES

To validate the effectiveness of each component in IntTravel model, we conduct extensive ablation studies. We compare the **full version** of IntTravel against several variants with specific modules removed:

- **Ablation of TIP:** We evaluate the contribution of TIP module by ablating its core components in three variants: (1) *w/o J_k^{pre}* : J_k^{pre} is replaced with H^{pre} . (2) *w/o J_k^{res}* : J_k^{res} is replaced with H^{res} . (3) *w/o J_k^{pre} and J_k^{res}* : J_k^{pre} and J_k^{res} are replaced with H^{pre} and H^{res} , respectively. (4) *w/o TIP*: the whole TIP module is removed.
- **Ablation of TSG:** We investigate the two main mechanisms within TSG module by the following ablation settings: (1) *w/o hidden states*: removes the aggregation of intermediate

Table 5: Results of ablation experiments. For metrics, \uparrow indicates higher is better, and \downarrow indicates lower is better.

Model	“When” task		“How” task		“Where” task			“Via” task			
	Acc \uparrow	MAE \downarrow	Acc \uparrow	BCR \downarrow	HR@1 \uparrow	HR@5 \uparrow	CIR \downarrow	HR@1 \uparrow	HR@5 \uparrow	CIR \downarrow	
TIP	w/o J^{pre}	0.8327	8.031	<u>0.6752</u>	0.0733	0.6549	0.8548	0.2583	0.6577	0.8555	0.2561
	w/o J^{res}	<u>0.8329</u>	8.021	0.6732	0.0736	0.6539	0.8546	0.2588	0.6571	0.8556	<u>0.2558</u>
	w/o J^{pre} and J^{res}	0.8328	8.024	0.6731	<u>0.0730</u>	0.6566	<u>0.8552</u>	0.2576	<u>0.6582</u>	<u>0.8558</u>	<u>0.2558</u>
	w/o TIP	<u>0.8329</u>	8.023	0.6748	0.0734	0.6488	0.8542	0.2625	0.6545	0.8548	0.2581
TSG	w/o hidden states	0.8328	8.025	0.6718	0.0740	0.6535	0.8549	0.2585	0.6544	0.8550	0.2578
	w/o task gating	0.8328	8.028	0.6730	0.0742	0.6532	0.8546	0.2594	0.6562	0.8544	0.2573
TSF	w/o TSF	<u>0.8329</u>	<u>8.019</u>	0.6723	0.0733	0.6259	0.8464	0.2696	0.6237	0.8460	0.2715
Full version		0.8330	8.016	0.6756	0.0724	0.6582	0.8556	0.2560	0.6592	0.8561	0.2552

hidden states from the HSTU layers, relying exclusively on the final layer’s output. (2) *w/o task gating*: disable the task-specific gating mechanism, forcing all tasks to share the same fused representation without differentiation. The input of TSF module is the average pooling of all HSTU layers’ outputs.

- **Ablation of TSF:** *w/o TSF*: the entire TSF module is replaced with an MLP.

The results presented in Table 5 confirm the critical contribution of each proposed module. The most significant performance degradation is observed when the TSF module is removed entirely. This indicates that dynamically generating customized parameters for each specific task-user scenario is of vital importance. Furthermore, the results highlight the importance of the TIP and TSG modules. Removing TIP impairs the model’s ability to propagate and preserve task-relevant information across layers, leading to a consistent performance drop. Similarly, ablating the gating mechanism within TSG underscores the necessity of its selective filtering capability. The full version model effectively combines these modules to achieve the best overall results.

6.5 SCALING LAWS

To investigate the scaling capability of our model, we trained several models, with depths ranging from 1 layer to 80 layers. The performance of these variants was evaluated with positive metrics of all four tasks (Acc for “When” and “How” tasks, and HR@1 for “Where” and “Via” tasks), as well as the total loss. The results are visualized in Figure 3, revealing a strong and consistent scaling trend. As the model depth increases from 1 to 80 layers, performance on all metrics steadily improves. There is no sign of performance decrease even at very deep configurations like 80 layers, which is often a challenge for complex models. This demonstrates the excellent scaling capability of proposed architecture.

6.6 ONLINE A/B TEST

An online A/B test was conducted for IntTravel to evaluate the proposed model against the current production baseline. Each experimental variant was allocated 5% of total user traffic. The results showed that IntTravel led to a **1.09% increase** in CTR, demonstrating its significant value in a real-world production environment.

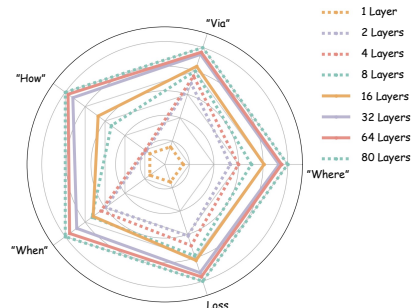


Figure 3: Scaling effects with varying layers. All plotted points are computed after min–max normalization. Task accuracy increases outward while loss decreases outward.

7 CONCLUSION

In this paper, we addressed a critical limitation in travel recommendation research: the lack of large-scale, public datasets for holistic journey planning. To bridge this gap, we introduced **IntTravel**, a massive real-world dataset containing over 4 billion user interactions. Built upon this dataset, we proposed a novel, decoder-only generative framework designed to handle multiple tasks. Our framework effectively balances shared knowledge with task-specific needs through three key modules: Task-Guided Information Persistence (TIP), Task-Specific Selective Gating (TSG), and Task-Aware Scenario Factorization (TSF). Extensive experiments demonstrate that our model achieves state-of-the-art performance on both the IntTravel dataset and another non-travel benchmark, proving its effectiveness and generalizability. The practical value of our work is confirmed by its successful deployment in the Amap application, where it led to a significant 1.09% increase in CTR.

REFERENCES

Kingma DP Ba J Adam et al. A method for stochastic optimization. *arXiv preprint arXiv:1412.6980*, 1412(6), 2014. 10

Rich Caruana. Multitask learning. *Machine learning*, 28(1):41–75, 1997. 3

Zhiyuan Cheng, James Caverlee, Kyumin Lee, and Daniel Sui. Exploring millions of footprints in location sharing services. In *Proceedings of the International AAAI Conference on Web and Social Media*, volume 5, pp. 81–88, 2011. 1, 2, 3

Eunjoon Cho, Seth A Myers, and Jure Leskovec. Friendship and mobility: user movement in location-based social networks. In *Proceedings of the 17th ACM SIGKDD international conference on Knowledge discovery and data mining*, pp. 1082–1090, 2011. 1, 2, 3

Jiaxin Deng, Shiyao Wang, Kuo Cai, Lejian Ren, Qigen Hu, Weifeng Ding, Qiang Luo, and Guorui Zhou. Onerec: Unifying retrieve and rank with generative recommender and iterative preference alignment, 2025a. URL <https://arxiv.org/abs/2502.18965>. 4

Jiaxin Deng, Shiyao Wang, Kuo Cai, Lejian Ren, Qigen Hu, Weifeng Ding, Qiang Luo, and Guorui Zhou. Onerec: Unifying retrieve and rank with generative recommender and iterative preference alignment. *arXiv preprint arXiv:2502.18965*, 2025b. 2

Shijie Geng, Shuchang Liu, Zuohui Fu, Yingqiang Ge, and Yongfeng Zhang. Recommendation as language processing (rlp): A unified pretrain, personalized prompt & predict paradigm (p5). In *Proceedings of the 16th ACM conference on recommender systems*, pp. 299–315, 2022. 3

Ruidong Han, Bin Yin, Shangyu Chen, He Jiang, Fei Jiang, Xiang Li, Chi Ma, Mincong Huang, Xiaoguang Li, Chunzhen Jing, et al. Mtgr: Industrial-scale generative recommendation framework in meituan. In *Proceedings of the 34th ACM International Conference on Information and Knowledge Management*, pp. 5731–5738, 2025. 6

Yilun Hao, Yongchao Chen, Yang Zhang, and Chuchu Fan. Large language models can solve real-world planning rigorously with formal verification tools. In *Proceedings of the 2025 Conference of the Nations of the Americas Chapter of the Association for Computational Linguistics: Human Language Technologies (Volume 1: Long Papers)*, pp. 3434–3483, 2025. 3

Peibo Li, Maarten de Rijke, Hao Xue, Shuang Ao, Yang Song, and Flora D Salim. Large language models for next point-of-interest recommendation. In *Proceedings of the 47th International ACM SIGIR Conference on Research and Development in Information Retrieval*, pp. 1463–1472, 2024. 2

Enze Liu, Bowen Zheng, Cheng Ling, Lantao Hu, Han Li, and Wayne Xin Zhao. Generative recommender with end-to-end learnable item tokenization. In *Proceedings of the 48th International ACM SIGIR Conference on Research and Development in Information Retrieval*, pp. 729–739, 2025. 3

Jiaqi Ma, Zhe Zhao, Xinyang Yi, Jilin Chen, Lichan Hong, and Ed H Chi. Modeling task relationships in multi-task learning with multi-gate mixture-of-experts. In *Proceedings of the 24th ACM SIGKDD international conference on knowledge discovery & data mining*, pp. 1930–1939, 2018. 3

Diego Monti, Enrico Palumbo, Giuseppe Rizzo, Raphaël Troncy, Thibault Ehrhart, and Maurizio Morisio. Semantic trails of city explorations: How do we live a city. *arXiv preprint arXiv:1812.04367*, 2018. 1, 2

Shashank Rajput, Nikhil Mehta, Anima Singh, Raghunandan Hulikal Keshavan, Trung Vu, Lukasz Heldt, Lichan Hong, Yi Tay, Vinh Tran, Jonah Samost, et al. Recommender systems with generative retrieval. *Advances in Neural Information Processing Systems*, 36:10299–10315, 2023a. 4

Shashank Rajput, Nikhil Mehta, Anima Singh, Raghunandan Hulikal Keshavan, Trung Vu, Lukasz Heldt, Lichan Hong, Yi Tay, Vinh Tran, Jonah Samost, et al. Recommender systems with generative retrieval. *Advances in Neural Information Processing Systems*, 36:10299–10315, 2023b. 2

Xiang-Rong Sheng, Liqin Zhao, Guorui Zhou, Xinyao Ding, Binding Dai, Qiang Luo, Siran Yang, Jingshan Lv, Chi Zhang, Hongbo Deng, et al. One model to serve all: Star topology adaptive recommender for multi-domain ctr prediction. In *Proceedings of the 30th ACM International Conference on Information & Knowledge Management*, pp. 4104–4113, 2021. 3, 9

Liangcai Su, Junwei Pan, Ximei Wang, Xi Xiao, Shijie Quan, Xihua Chen, and Jie Jiang. Stem: unleashing the power of embeddings for multi-task recommendation. In *Proceedings of the AAAI conference on artificial intelligence*, volume 38, pp. 9002–9010, 2024. 3, 9

Hongyan Tang, Junning Liu, Ming Zhao, and Xudong Gong. Progressive layered extraction (ple): A novel multi-task learning (mtl) model for personalized recommendations. In *Proceedings of the 14th ACM conference on recommender systems*, pp. 269–278, 2020. 3, 9

Dongsheng Wang, Yuxi Huang, Shen Gao, Yifan Wang, Chengrui Huang, and Shuo Shang. Generative next poi recommendation with semantic id. In *Proceedings of the 31st ACM SIGKDD Conference on Knowledge Discovery and Data Mining V. 2*, pp. 2904–2914, 2025a. 2

Jiawei Wang, Renhe Jiang, Chuang Yang, Zengqing Wu, Makoto Onizuka, Ryosuke Shibusaki, Noboru Koshizuka, and Chuan Xiao. Large language models as urban residents: An llm agent framework for personal mobility generation. *Advances in Neural Information Processing Systems*, 37:124547–124574, 2024. 2

Kaimin Wang, Yuanzhe Shen, Changze Lv, Xiaoqing Zheng, and Xuan-Jing Huang. Triptailor: A real-world benchmark for personalized travel planning. In *Findings of the Association for Computational Linguistics: ACL 2025*, pp. 9705–9723, 2025b. 3

Xu Wang, Jiangxia Cao, Zhiyi Fu, Kun Gai, and Guorui Zhou. Home: Hierarchy of multi-gate experts for multi-task learning at kuaishou. In *Proceedings of the 31st ACM SIGKDD Conference on Knowledge Discovery and Data Mining V. 1*, pp. 2638–2647, 2025c. 9

Zhipeng Wei, Kuo Cai, Junda She, Jie Chen, Minghao Chen, Yang Zeng, Qiang Luo, Wencong Zeng, Ruiming Tang, Kun Gai, et al. Oneloc: Geo-aware generative recommender systems for local life service. *arXiv preprint arXiv:2508.14646*, 2025. 2

Jian Xie, Kai Zhang, Jiangjie Chen, Tinghui Zhu, Renze Lou, Yuandong Tian, Yanghua Xiao, and Yu Su. Travelplanner: a benchmark for real-world planning with language agents. In *Proceedings of the 41st International Conference on Machine Learning*, pp. 54590–54613, 2024. 3

Senrong Xu, Liangyue Li, Yuan Yao, Zulon Chen, Han Wu, Quan Lu, and Hanghang Tong. Musenet: Multi-scenario learning for repeat-aware personalized recommendation. In *Proceedings of the Sixteenth ACM International Conference on Web Search and Data Mining*, pp. 517–525, 2023. 9

Songpei Xu, Shijia Wang, Da Guo, Xianwen Guo, Qiang Xiao, Bin Huang, Guanlin Wu, and Chuanjiang Luo. Climber: Toward efficient scaling laws for large recommendation models. In *Proceedings of the 34th ACM International Conference on Information and Knowledge Management*, pp. 6193–6200, 2025. [3](#)

Bencheng Yan, Pengjie Wang, Kai Zhang, Feng Li, Hongbo Deng, Jian Xu, and Bo Zheng. Apg: Adaptive parameter generation network for click-through rate prediction. *Advances in Neural Information Processing Systems*, 35:24740–24752, 2022. [9](#)

Huimin Yan, Longfei Xu, Junjie Sun, Ni Ou, Wei Luo, Xing Tan, Ran Cheng, Kaikui Liu, and Xiangxiang Chu. Intsr: An integrated generative framework for search and recommendation. *arXiv preprint arXiv:2509.21179*, 2025. [2](#), [4](#), [5](#), [6](#)

Dingqi Yang, Daqing Zhang, Vincent W Zheng, and Zhiyong Yu. Modeling user activity preference by leveraging user spatial temporal characteristics in lbsns. *IEEE Transactions on Systems, Man, and Cybernetics: Systems*, 45(1):129–142, 2014. [1](#), [2](#), [3](#)

Dingqi Yang, Daqing Zhang, and Bingqing Qu. Participatory cultural mapping based on collective behavior data in location-based social networks. *ACM Transactions on Intelligent Systems and Technology (TIST)*, 7(3):1–23, 2016. [1](#), [2](#)

Dingqi Yang, Bingqing Qu, Jie Yang, and Philippe Cudre-Mauroux. Revisiting user mobility and social relationships in lbsns: a hypergraph embedding approach. In *The world wide web conference*, pp. 2147–2157, 2019. [1](#), [2](#)

Jiahao Yu, Yihai Duan, Longfei Xu, Chao Chen, Shuliang Liu, Kaikui Liu, Fan Yang, Xiangxiang Chu, and Ning Guo. Dsfnet: Learning disentangled scenario factorization for multi-scenario route ranking. In *Companion Proceedings of the ACM on Web Conference 2025*, pp. 567–576, 2025. [8](#)

Guanghu Yuan, Fajie Yuan, Yudong Li, Beibei Kong, Shujie Li, Lei Chen, Min Yang, Chenyun Yu, Bo Hu, Zang Li, et al. Tenrec: A large-scale multipurpose benchmark dataset for recommender systems. *Advances in Neural Information Processing Systems*, 35:11480–11493, 2022. [8](#), [9](#)

Jiaqi Zhai, Lucy Liao, Xing Liu, Yueming Wang, Rui Li, Xuan Cao, Leon Gao, Zhaojie Gong, Fangda Gu, Jiayuan He, et al. Actions speak louder than words: trillion-parameter sequential transducers for generative recommendations. In *Proceedings of the 41st International Conference on Machine Learning*, pp. 58484–58509, 2024a. [4](#), [6](#)

Jiaqi Zhai, Lucy Liao, Xing Liu, Yueming Wang, Rui Li, Xuan Cao, Leon Gao, Zhaojie Gong, Fangda Gu, Jiayuan He, et al. Actions speak louder than words: Trillion-parameter sequential transducers for generative recommendations. In *International Conference on Machine Learning*, pp. 58484–58509. PMLR, 2024b. [2](#)

Qianqian Zhang, Xinru Liao, Quan Liu, Jian Xu, and Bo Zheng. Leaving no one behind: A multi-scenario multi-task meta learning approach for advertiser modeling. In *Proceedings of the Fifteenth ACM International Conference on Web Search and Data Mining*, pp. 1368–1376, 2022. [3](#), [9](#)

Bowen Zheng, Yupeng Hou, Hongyu Lu, Yu Chen, Wayne Xin Zhao, Ming Chen, and Ji-Rong Wen. Adapting large language models by integrating collaborative semantics for recommendation. In *2024 IEEE 40th International Conference on Data Engineering (ICDE)*, pp. 1435–1448. IEEE, 2024. [3](#)

Jie Zhou, Xianshuai Cao, Wenhao Li, Lin Bo, Kun Zhang, Chuan Luo, and Qian Yu. Hinet: Novel multi-scenario & multi-task learning with hierarchical information extraction. In *2023 IEEE 39th International Conference on Data Engineering (ICDE)*, pp. 2969–2975. IEEE, 2023. [3](#), [9](#)

Defa Zhu, Hongzhi Huang, Zihao Huang, Yutao Zeng, Yunyao Mao, Banggu Wu, Qiyang Min, and Xun Zhou. Hyper-connections. In *The Thirteenth International Conference on Learning Representations*. [6](#)

A INTTRAVEL DATASET: FIELDS, STATISTICS, AND EXAMPLES

A.1 INFORMATION OF POIs

The IntTravel dataset proposed in this paper contains 7,291,872 POIs distributed across several major cities in China. Each POI is described by the following fields (see data examples in Table 6):

- **POI ID:** A unique identifier assigned to each POI. These IDs are anonymized by randomly shuffling the original identifiers and re-indexing them from 0.
- **Normalized score (Nscore):** A score ranging from 0 to 1 that reflects the overall popularity of a POI. This score is derived from multiple factors, including interaction frequency. The specific calculation formula is not disclosed, and users can directly treat this score as a popularity-like feature.
- **Geographic ID (GID):** An identifier for the geographic block where the POI is located. Similar to POI IDs, these block IDs have been anonymized and re-indexed. The adjacency of IDs does not imply geographic proximity between blocks. However, POIs sharing the same geographic ID can be considered geographically close.
- **Category ID (CID):** An integer identifier representing the POI’s category. For data protection purposes, the original category labels have been converted into numerical IDs starting from 0.
- **Administrative Region ID (ARID):** An integer identifier for the administrative region of the POI. Similarly, the original region identifiers have been transformed into numerical IDs to preserve privacy.
- **Coordinates:** The spatial coordinates of the POI. The provided (x, y) coordinates represent anonymized spatial locations projected onto a 2D Cartesian plane. These coordinates are not standard longitude/latitude but are designed to preserve the relative relationship of the original data.

A.2 USER PROFILES

The IntTravel dataset contains 162,815,861 users, each described by the following fields. Table 7 provides some examples of the user profile data.

- **User ID:** A unique identifier assigned to each user. To ensure anonymity, these IDs were generated by shuffling the original identifiers and re-indexing them from 0.
- **User Profile Features:** A set of six distinct profile features. To protect user privacy, both the original feature names and their raw values have been anonymized. Each feature has been transformed into a discrete integer ID. Some feature values may be missing. Figure 4 illustrates the proportion of valid (non-missing) values for each of the six profile features.

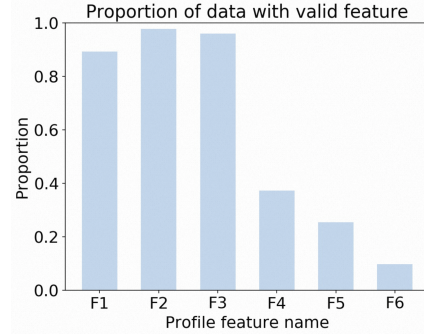


Figure 4: Proportion of valid data per feature in user profile data of IntTravel. “F1” is short for “Feature 1”.

A.3 USER INTERACTION BEHAVIORS

The IntTravel dataset also include 4,129,827,011 user interaction events. Each event is characterized by the following fields, with examples provided in Table 8.

- **User ID:** The identifier of the user who performed the interaction. This ID corresponds directly to the “User ID” in the user dataset.
- **Timestamp:** A value in milliseconds indicating when the interaction occurred. To protect privacy, these values have been processed and are not the raw timestamps, but their relative order is preserved.

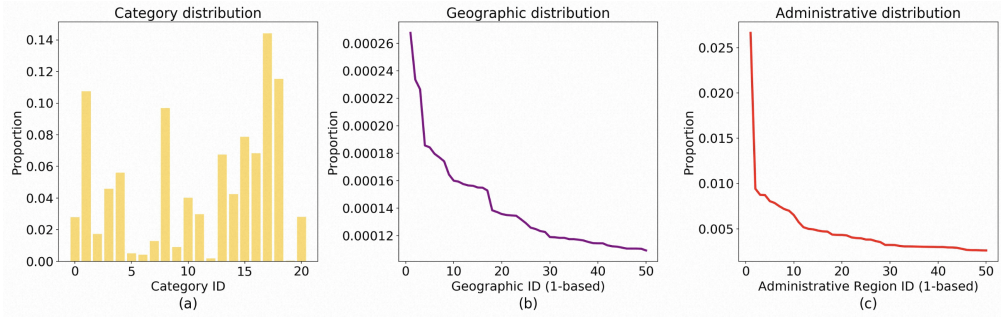


Figure 5: POI distribution analysis: categorical, administrative, and geographic dimensions. For readability, (b) and (c) only display the top 50 GIDs and ARIDs with the highest number of POIs. Both the geographic and administrative distributions exhibit a long-tail pattern.

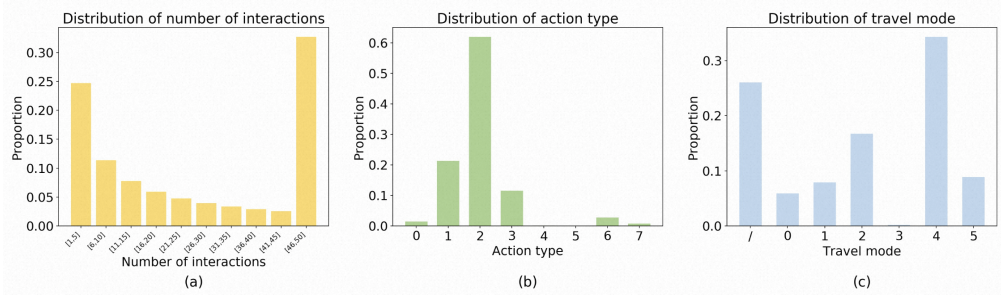


Figure 6: Distribution of user behaviors: number of times, action types, and travel modes. The slash (/) indicates no travel modes information is included in the data.

- **Action Type:** An integer ID representing the type of user behavior (e.g., a click or route planning). For data protection, the original operation names have been anonymized and converted into these numerical IDs.
- **POI ID:** The identifier of the POI involved in the interaction. This ID corresponds to an entry in the POI dataset.
- **Geographic ID (GID):** The ID of the geographic block where the user was located when the interaction occurred. This ID shares the same encoding system as the GIDs in the POI dataset.
- **Administrative Region ID (ARID):** The ID of the administrative region where the user was located when the interaction occurred. Similarly, this ID shares the same encoding system as the ARIDs in the POI dataset.
- **Weather:** An integer ID representing the weather condition at the time of the interaction. The original weather descriptions have been converted into numerical IDs.
- **Travel Mode:** An integer ID representing the user’s chosen mode of travel. The original information has been anonymized for privacy. This field may be null for some records.
- **Via POI ID:** The identifier for a way-point POI added by the user, which also corresponds to an entry in the POI dataset. This field may be null, as not all interactions involve way-points.

We capped the number of historical user interactions at 50. Figure 6 depicts the distribution of user behavior along several dimension.

Table 6: Data examples of POI information.

POI ID	Nscore	GID	CID	ARID	Coordinates
0	0.436961	25556599	8	353	21541.38, -16385.12
1	0.389202	5901606	1	2089	21543.91, -16389.45
2	0.190659	17952948	17	3192	21520.76, -16412.67

Table 7: Examples of user data, including user IDs and anonymized profile features. “F1” is short for “Feature 1”. The slash (/) denotes a missing value.

User ID	F1	F2	F3	F4	F5	F6
108452457	0	0	2	/	2	0
108452458	0	0	6	5	3	/
108452459	1	1	1	/	/	/

B EVALUATION METRICS

To comprehensively evaluate the performance of our model, we define a set of specific metrics for each task. These metrics include both positive indicators (where higher is better) and negative indicators (where lower is better) to provide a holistic view of the model’s capabilities.

B.1 “WHEN” TASK

Positive: **Accuracy (Acc)** measures the percentage of predictions that exactly match the ground-truth departure time:

$$\text{Acc} = \frac{1}{|\mathcal{T}|} \sum_{i \in \mathcal{T}} \mathbb{I}(\hat{y}_i = y_i) \quad (18)$$

where \mathcal{T} is the test set, y_i is the ground-truth departure time, \hat{y}_i is the predicted result, and $\mathbb{I}(\cdot)$ is the indicator function.

Negative: **Mean Absolute Error (MAE)** calculates the average absolute difference between predicted and actual values, reflecting the overall prediction bias.

$$\text{MAE} = \frac{1}{|\mathcal{T}|} \sum_{i \in \mathcal{T}} |\hat{y}_i - y_i| \quad (19)$$

B.2 “HOW” TASK

Positive: **Accuracy (Acc)** is the proportion of correctly predicted travel modes.

Negative: **Bad Case Rate (BCR)** measures the rate of predictions leading to bad user experience. Mobile navigation applications typically display only three travel mode recommendations on the primary screen. Failing to include the user’s preferred option in this top-3 set forces them to take extra steps, resulting in a poor user experience. Based on this observation, we calculate BCR as the **Top-3 Miss Rate**.

B.3 “WHERE” AND “VIA” TASKS

Positive: **HitRate@N** measures whether the ground-truth POI is included in the top-N recommended items. It is a standard metric for evaluating ranking quality.

$$\text{HitRate@N} = \frac{1}{|\mathcal{T}|} \sum_{i \in \mathcal{T}} \mathbb{I}(y_i \in \text{TopN}(\hat{R}_i)) \quad (20)$$

where \hat{R}_i is the ranked list of candidate POIs for the i -th sample, and $\text{TopN}(\cdot)$ returns the top-N items from that list.

Table 8: Examples of user interaction log data. Each row represents a single interaction event with its associated context. The slash (/) denotes a missing value.

User ID	Timestamp	Action Type	Target POI ID	GID	ARID	Weather	Travel Mode	Via POI ID
70588810	4731399094	2	1233656	24276681	2778	14	1	/
70588810	155476000	3	908725	35758646	213	9	2	/
77276360	6288157866	7	5852976	46698773	2883	20	4	5403246

Table 9: Results of ablation experiments on task and task-related features. For metrics, \uparrow indicates higher is better, and \downarrow indicates lower is better. The slash (/) indicates metrics not applicable to the given model.

Model	“When” task		“How” task		“Where” task			“Via” task		
	Acc \uparrow	MAE \downarrow	Acc \uparrow	BCR \downarrow	HR@1 \uparrow	HR@5 \uparrow	CIR \downarrow	HR@1 \uparrow	HR@5 \uparrow	CIR \downarrow
w/o “When”	/	/	0.6650	0.0754	0.6469	0.8520	0.2766	0.6546	0.8550	0.2724
w/o “How”	0.8329	8.021	/	/	0.6569	0.8545	0.2692	0.6588	0.8553	0.2704
w/o “Where”	0.8328	8.023	0.6697	0.0752	/	/	/	0.5325	0.7997	0.3763
w/o “Via”	0.8328	8.027	0.6747	0.0727	0.6509	0.8538	0.2701	/	/	/
Full version	0.8330	8.016	0.6756	0.0724	0.6582	0.8556	0.2560	0.6592	0.8561	0.2552

Negative: **Category Inconsistency Rate (CIR)**. Since recommending a POI from the same category as the ground truth can also be reasonable, CIR measures the rate at which the top-1 prediction is neither the ground-truth POI nor belongs to the same category as the ground truth:

$$\text{CIR} = \frac{1}{|\mathcal{T}|} \sum_{i \in \mathcal{T}} \mathbb{I}(\hat{y}_i^{(1)} \neq y_i \wedge \text{Cate}(\hat{y}_i^{(1)}) \neq \text{Cate}(y_i)) \quad (21)$$

where $\hat{y}_i^{(1)}$ is the top-1 predicted POI, and $\text{Cate}(\text{POI})$ denotes the category of a given POI.

C ANALYSIS OF INTER-TASK CORRELATION

To investigate the inter-dependencies among the four travel tasks, we conduct a comprehensive ablation study on tasks and task-related features. We create four variants of our model, each designed to exclude one specific task and its associated input features:

- w/o “When”: all timestamp-related features and the corresponding “When” task are removed.
- w/o “How”: travel mode features and its prediction task are omitted.
- w/o “Where”: the token embedding on I positions is replaced with an all-zero vector; besides, the “Where” task is removed.
- w/o “Via”: both way-point data and the associated via-point prediction task are removed.

The results are presented in Table 9. The full version model consistently outperforms all ablation variants, indicating that each task provides valuable context that benefits the others. The most significant performance decrease is observed in the w/o “Where” variant. Removing destination information causes a significant drop in the performance of the “Via” task (e.g., HR@1 declines from 0.6592 to 0.5325). This highlights a strong logical dependency, as predicting a route is inherently difficult without knowing the destination. Removing other tasks like w/o “How” or w/o “Via” also leads to a noticeable, although smaller, performance decline across other metrics. These findings validate our multi-task approach, proving that the tasks are not independent but mutually beneficial.